Available online at www.sciencedirect.com
ScienceDirect
Journal of Nuclear Materials 367–370 (2007) 876–881
journal of nuclear materials
www.elsevier.com/locate/jnucmat

Diffusional behavior of tritium in V–4Cr–4Ti alloy

K. Hashizume [a,*], J. Masuda [a], T. Otsuka [a], T. Tanabe [a], Y. Hatano [b,1], Y. Nakamura [c,2], T. Nagasaka [c,2], T. Muroga [c,2]

[a] *Interdisciplinary Graduate School of Engineering Sciences, Kyushu University, 6-10-1 Hakozaki, Fukuoka 812-8581, Japan*
[b] *Hydrogen Isotope Research Center, The University of Toyama, Toyama 930-8555, Japan*
[c] *National Institute for Fusion Science, Toki, Gifu 509-5292, Japan*

Abstract

Tritium diffusion behavior in a V–4Cr–4Ti (NIFS-Heat-2) alloy has been examined with a tritium tracer technique. Firstly, a small amount of tritium (T) was implanted into the specimen surface, and then the specimen was diffusion-annealed at temperatures ranging from 373 K to 573 K. The diffusion depth profile of T in the specimen was measured with a tritium imaging plate (IP) technique to determine the diffusion coefficient. The obtained diffusion coefficient of tritium in V–4Cr–4Ti is expressed as

$$D_t\ (\mathrm{cm}^2/\mathrm{s}) = (7.5 \pm 0.2) \times 10^{-4} \exp(-0.13(\mathrm{eV})/kT),$$

which is lower than that in pure vanadium, and is comparable with literature values of protium in a V–4Ti alloy taking the isotope mass effect into consideration.

1. Introduction

Low activation vanadium alloys have been developed as good candidate structural materials of a nuclear fusion reactor [1,2], and their material properties have been examined from various aspects. Tritium retention and permeation in the alloys are also important concerns and the diffusion coefficient of tritium is one of the key parameters to be evaluated. For pure V, diffusion coefficients of hydrogen isotopes and trapping effects of some alloying elements have been examined [3–7]. However, only limited data are available for the newly developed alloys.

In the present study, we have examined hydrogen diffusion behavior in a V–4Cr–4Ti (NIFS-Heat-2) alloy [2,8] applying a tritium tracer technique, in which a small amount of tritium (T) together with hydrogen (H) was first implanted into the specimen surface. The specimen was diffusion-annealed at a temperature from 373 K to 523 K, and then the diffusion depth profile of T in the specimen was measured to determine the diffusion coefficient. The tritium imaging plate (IP) technique was used to obtain the diffusion profile of T. In this technique, the diffusion-annealed specimen was exposed to IP for a certain time duration and finally processed by an imaging plate reader to get intensity profiles

* Corresponding author. Tel./fax: +81 92 642 3796.
E-mail address: hashi@nucl.kyushu-u.ac.jp (K. Hashizume).
[1] Tel.: +81 76 445 6928; fax: +81 76 445 6931.
[2] Tel.: +81 572 58 2164; fax: +81 572 58 2618.

0022-3115/$ - see front matter © 2007 Elsevier B.V. All rights reserved.
doi:10.1016/j.jnucmat.2007.03.239

of photo-stimulated luminescence (PSL) corresponding to the diffusion profile of T.

The obtained diffusion coefficients of tritium in V–4Cr–4Ti alloy are compared with literature values of hydrogen isotopes dissolved in V alloys, and diffusional behavior of tritium is discussed in terms of trapping effects due to alloying elements.

2. Experimental

V–4Cr–4Ti rods (NIFS-Heat-2, 50 mm long, 2 mm in diameter), which were heated in a vacuum (10^{-5} Pa) at 1273 K for 2 h, were used as specimens for a diffusion experiment. By means of applying a glow discharge method [9], tritium was implanted into the front end surface of the specimens which was mechanically polished with abrasive papers and finished with 0.3 μm Al_2O_3 powder. In this method, the specimen was set in a round hole (2.1 mm in diameter) bored in a stainless steel electrode of a discharge tube, as shown in Fig. 1. The discharge was made by applying an altering electric potential of 4 kV at 60 Hz between two electrodes in hydrogen gas of 30 Pa including T with T/H $\sim 10^{-6}$ and maintained for 40 min. During the discharge, the lower part of the discharge tube was immersed in a liquid N_2 filled Dewar flask in order to prevent temperature rise of the specimen as well as tritium diffusion in it. Accordingly, ca. 10^{-6} mole of hydrogen (10^{-12} mole of tritium) impinged on the end surface of the specimens. The details of this discharge implantation method have been given elsewhere [9].

After the tritium implantation, the specimen surfaces, except the implanted front end surface, were examined to determine whether they were contaminated by tritium with an imaging plate (IP). Any contaminated surfaces were removed with abrasive papers. Then, the specimens were diffusion-annealed in a vacuum (10^{-5} Pa) at a temperature ranging from 373 K to 573 K. After the diffusion annealing, the specimen was cooled down to room temperature and its surface oxide layer was removed. Then, the specimen was exposed to IP (FUJIFILM BAS-TR2025) for 24 h at liquid N_2 temperature and the photo-stimulated luminescence (PSL) intensity distribution was measured with an IP reader (FUJIFILM BAS 2500). The diffusion coefficient of tritium in the specimen was determined from the PSL intensity distribution on a basis of the one-dimensional diffusion equation.

3. Results and discussion

It is well known that IP has a wide dynamic range for surface radiation activity, and the PSL intensity varies proportionally with adsorbed energy in IP over a wide adsorbed energy range [10–12]. IP has been successfully applied for the determination of tritium diffusion coefficients in zirconium and its alloys by the present research group [13].

In the present work, tritium was implanted at the front end of the rod-shaped specimen, and tritium diffusion along the rod (designated as the x coordinate) was examined by IP, with the implanted front

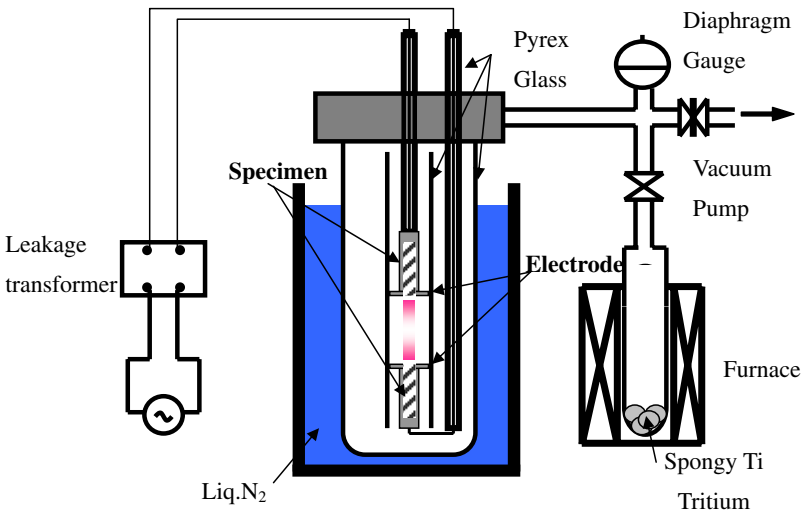

Fig. 1. Schematic apparatus for the tritium glow discharge implantation method with glow discharge of tritiated hydrogen gas.

end being the origin of the x axis as shown in Fig. 2(a). In the case of the rod-shaped specimen, the contact area of the specimen to the flat IP is rather small, so that reliability of the PSL profile along the specimen should be rather low. Therefore, the specimens were mechanically ground with abrasive papers up to the thickness of 500–1000 μm to get a flat surface, as shown in Fig. 2(a). After the grinding, the specimen was rinsed with acetone in an ultrasonic bath. In this grinding and rinsing process, tritium on the specimen surface should be removed, but the oxide layers formed immediately prevented further tritium release. The initial distribution of tritium in the specimen given by the tritium image is shown as the inset in Fig. 2(b). Although the brighter area extends to the left side of the specimen owing to the exposure of IP with the beta rays traveling in air from the end surface of the specimen, there is no indication of tritium diffusion into the specimen. Thus, tritium existed as a thin diffusion source before the diffusion annealing. During the diffusion annealing, leakage of hydrogen gas from the top edge surfaces perpendicular to the diffusion direction was prohibited by the surface oxide layers. The barrier effect of the surface oxide is limited to temperatures below 573 K, above which the surface oxide disappeared because oxygen is dissolved into the bulk. As a result, tritium release out of the specimen started above 573 K, and the release rate increased rapidly above 623 K. Hence the measurements were limited to temperatures below 573 K. During the diffusion annealing, rather large amounts of oxygen uptake would make thicker oxide layers, by which the escape of tritium beta rays could be prohibited and/or hydrogen exhausted because hydrogen solubility in the oxide layer is small. Since the escaping depth of tritium beta rays from V is as small as ca. 2 μm, the PSL value might not well reflect tritium concentration in the bulk, if the surface was covered by thick oxide. Therefore, as mentioned in Section 2, the thick surface oxide layer on the specimen was removed with the abrasive paper before the specimen was exposed to IP.

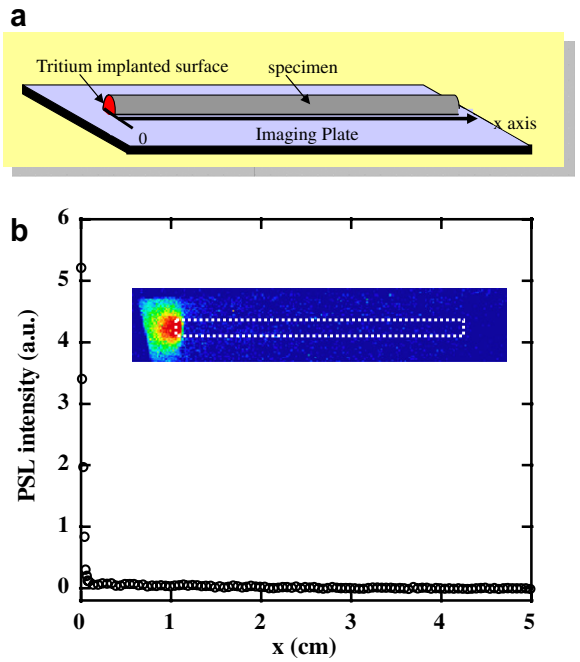

Fig. 2. (a) Configuration of specimen and IP during exposure and coordinates on IP for measurement of depth profile of tritium and (b) initial tritium distribution profile of a specimen using the imaging plate technique after tritium implantation with the glow discharge method.

Fig. 3(a) shows the tritium image (inset) and digitized profile along the diffusion direction just after a diffusion annealing at 523 K for 1.5 h. As seen in this image (inset), the brighter area extending to the left side of the specimen still remains. This means that part of the implanted tritium should be trapped with strong trapping sites induced by radiation damage of the specimen surface during the glow discharge implantation. In any case, the strongly trapped tritium is not diffusible, so that it should not affect the determination of the diffusion coefficient. In the present experiment, the tritium diffusion depth $(2D_t t)^{1/2}$ was adjusted to be 10 mm, which was sufficiently larger than the implanted region (20 μm) as was examined in the previous study [9] and shorter than the specimen length (50 mm), so that the tritium diffusion can be regarded to be one-dimensional semi-infinite. Under this condition, the solution of the one-dimensional diffusion equation yields the tritium concentration profile $C(x,t)$

$$C(x,t) = \frac{M}{\sqrt{\pi D_t t}} \exp\left(-\frac{x^2}{4D_t t}\right), \tag{1}$$

where M is the total amount of diffusing tritium initially existing as a thin film source, x the distance from the end surface, t the diffusion time and D_t the diffusion coefficient. Under the present experimental condition, the tritium concentration in the specimen is proportional to the PSL intensity

$$C(x,t) = A \times \mathrm{PSL}(x,t), \tag{2}$$

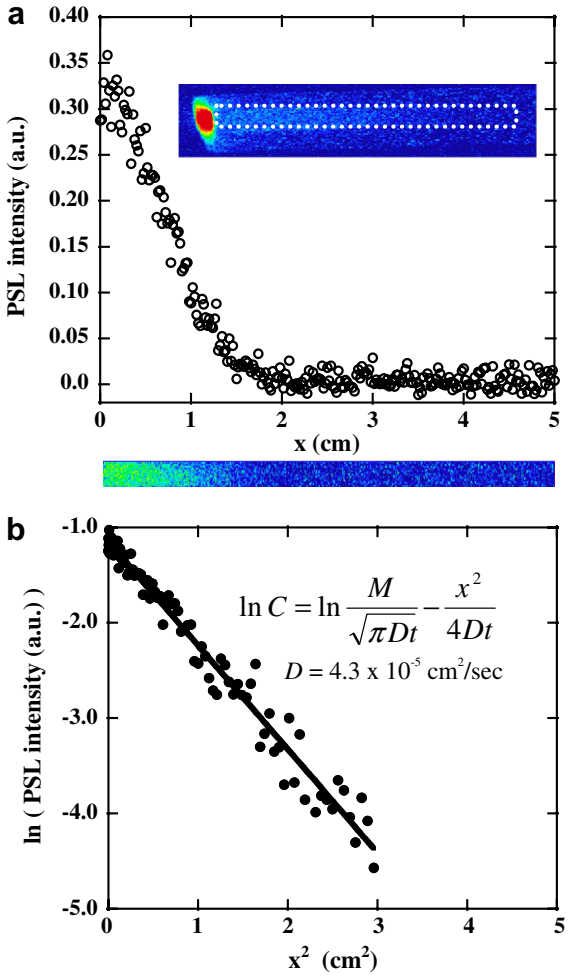

Fig. 3. (a) Example of tritium distribution profile of a specimen after diffusion annealing at 523 K for 1.5 h with imaging plate and (b) plot of ln(PSL) vs. x^2.

where A is a constant. The diffusion coefficient D_t can be determined from the PSL distribution by the least-squares fitting of Eqs. (1) and (2).

As seen in Fig. 3(a), the PSL data plotted against x are somewhat scattered. This scatter is believed to result from the areal resolution, which for the IP reader consists of an area of 50 μm × 50 μm, and the relatively low tritium concentration; i.e. the low surface activity measured in a small detection area should result in a relatively large uncertainty of the PSL intensity. In the present study, therefore, PSL values were smoothed, averaging over several resolution areas. Variation of the resolution area did not give much difference in the determined diffusion coefficient D_t and its experimental error. As seen in Fig. 3(b), the log(PSL) vs. x^2 plot indicates good linearity.

The diffusion coefficients obtained for tritium in the V–4Cr–4Ti specimen are listed in Table 1(a) and plotted against inverse temperature in Fig. 4(a). The diffusion coefficient of tritium in

Table 1(a)
Diffusion coefficient of tritium in V–4Cr–4Ti (NIFS-Heat-2)

Temperature (K)	D (cm^2/s)
373	$(1.35 \pm 0.03) \times 10^{-5}$
423	$(2.16 \pm 0.04) \times 10^{-5}$
523	$(4.29 \pm 0.07) \times 10^{-5}$
573	$(5.3 \pm 0.3) \times 10^{-5}$

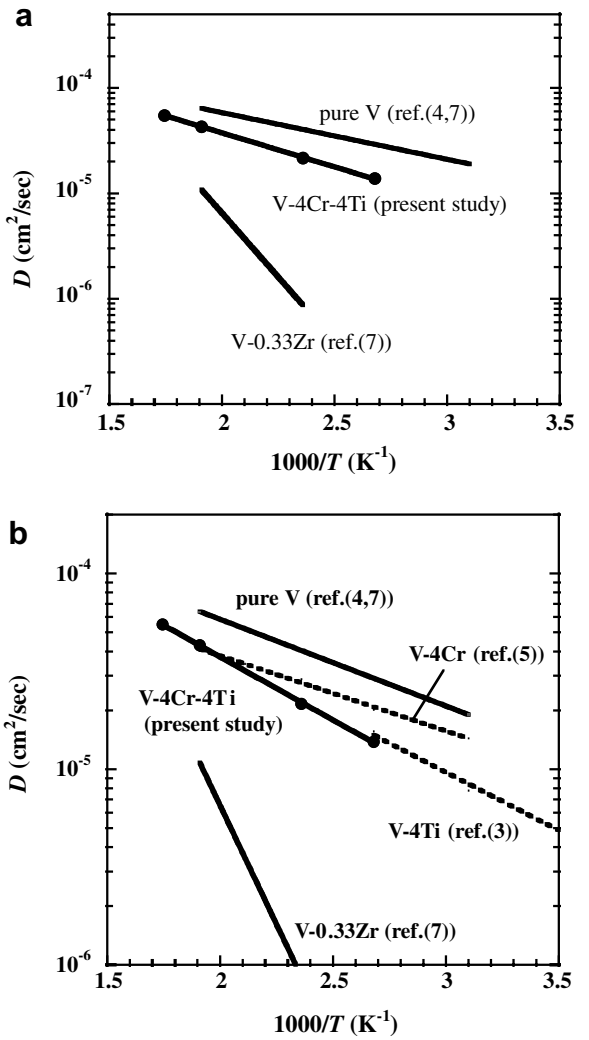

Fig. 4. (a) Diffusion coefficients of tritium in V–4Cr–4Ti and (b) comparison of tritium diffusion coefficient in V and V alloys with literature data.

Table 1(b)
Diffusion parameters of tritium diffusion coefficient in pure V and V alloys

	D_0 (cm^2/s)	E_a (eV)
V–4Cr–4Ti	7.5×10^{-4}	0.13
Pure V[a,b]	4.5×10^{-4}	0.09
V–0.33Zr[b]	2.3×10^{-1}	0.45

[a] Ref. [4].
[b] Ref. [7].

V–4Cr–4Ti shows a good Arrhenius relation, which is expressed as

$$D\ (\mathrm{cm}^2/\mathrm{s}) = (7.5\pm0.2)\times10^{-4}\exp(-0.13(\mathrm{eV})/kT). \quad (3)$$

Literature data [4,7] of D_t in pure V and V–Zr alloys are also depicted in Fig. 4(a) and listed in Table 1(b). As seen in Fig. 4(a), D_t of V–4Cr–4Ti is a little different (smaller) from that of pure V, but the difference is not so large as that of V–Zr alloy. In any case, this decrease of D_t and increase of the activation energy, in comparison with those of pure V, are believed to result from a trapping effect of tritium due to alloying elements of Cr and Ti.

We will now discuss the effect of alloying elements, Cr and Ti, in V–4Cr–4Ti. The diffusion coefficients of tritium in V–Cr and V–Ti alloys have not been reported, but those for protium and deuterium have been measured in a large composition region of each alloying element and trapping effects examined by several investigators [3,5,6]. Although diffusion data are somewhat scattered, the effect of alloying can be summarized as follows:

(a) Increasing content of alloying elements lowers the diffusion coefficient: reduction due to Ti alloying is more appreciable than that due to Cr.
(b) The activation energy of the diffusion coefficient, E_a, increases with increasing concentration of alloying elements: again Ti alloying is more appreciable than that due to Cr.
(c) Appreciable isotope mass effects in the diffusion coefficient and its activation energy are observed: $D(\mathrm{p}) > D(\mathrm{d})$ and $E_a(\mathrm{p}) < E_a(\mathrm{d})$.

Items (a) and (b) should mean that not only single substitutional Ti and Cr but di-, tri- and/or alloying element clusters play an important role as hydrogen trapping sites in V alloys. Actually, in the case of V–4Cr–4Ti, it has been reported that Ti rich phase and Ti compounds with carbon and oxygen precipitate in the alloy matrix, which depends on the heat treatment condition [14]. Such precipitates are also expected to influence the diffusion behavior of tritium. The isotope mass effect of the activation energy mentioned in item (c) means that the mass effect of the diffusion coefficient is not expressed on a basis of a simple mass effect on the pre-exponential or frequency factor. Nevertheless, the experimentally-obtained ratio of $D(\mathrm{p})/D(\mathrm{d})$ is approximately equal to $1/\sqrt{2}$. On a basis of these characteristics of the diffusional behavior of the hydrogen isotopes, the tritium diffusion coefficients are plotted again in Fig. 4(b), in which the data for protium in V–4Cr and V–4Ti alloys (dotted lines) are divided by a factor of $\sqrt{3}$. According to the above item (b), the data for V–4Cr–4Ti could be lower than that for V–4Ti or V–4Cr. As seen in Fig. 4(b), however, the data for V–4Cr–4Ti is very close to that for V–4Ti. Consequently, it might be safely concluded that the trapping effect of Ti on tritium diffusion is dominant for the case of V–4Cr–4Ti. This result also means that the trapping effects due to Ti and Cr should not be independent of each other. At the present stage, it is not clear whether the complex of Ti and Cr forms in V–4Cr–4Ti affects the diffusion behavior of tritium. In any case, the trapping mechanism of hydrogen isotopes in ternary alloys such as V–4Cr–4Ti is complicated, because of the formation of complexes and precipitates of alloying elements and/or other impurities. More systematic study is required to clarify the trapping mechanism of hydrogen isotopes by alloying elements.

4. Conclusions

1. The diffusion coefficient of tritium in V–4Cr–4Ti (NIFS-Heat-2) has been measured at temperatures ranging from 373 K to 573 K.
2. A tritium imaging plate (IP) technique has been successfully applied to measure the diffusion profile of tritium implanted into the specimens.
3. The diffusion coefficient obtained for tritium in V–4Cr–4Ti is expressed as

$$D\ (\mathrm{cm}^2/\mathrm{s}) = (7.5\pm0.2)\times10^{-4} \times \exp(-0.13(\mathrm{eV})/kT),$$

which is lower than that in pure vanadium, and is comparable with a literature value for protium in

a V–4Ti alloy taking a classical isotopic mass effect into consideration.

Acknowledgements

This work has been conducted with the support of the NIFS LHD Project Research Collaboration and partly through a Grand-in-Aid for Scientific Research (A, 17206092) from the Ministry of Education, Culture, Sports, Science and Technology of the Japanese Government.

References

[1] Y. Yano, M. Toda, H. Matsui, J. Nucl. Mater. 171–181 (1991) 779.
[2] T. Muroga, T. Nagasaka, K. Abe, V.M. Chernov, H. Matsui, D.L. Smith, Z.-Y. Xu, S.J. Zinkle, J. Nucl. Mater. 307–311 (2002) 547.
[3] S. Tanaka, H. Kimura, Trans. Jpn. Inst. Met. 20 (1979) 647.
[4] Zh. Qi, J. Völkl, R. Lässer, H. Wenzel, J. Phys. F: Met. Phys. 13 (1983) 2053.
[5] D.J. Pine, R.M. Cotts, Phys. Rev. B 28 (1983) 641.
[6] H. Nakajima, M. Yoshioka, M. Koiwa, Acta Metall. 35 (1987) 2731.
[7] K. Fujii, K. Hashizume, Y. Hatano, M. Sugisaki, J. Alloy. Compd. 270 (1998) 42.
[8] T. Muroga, T. Nagasaka, in: Fusion Energy 2000, 18th Conference Proceeding, Sorrento, October 2000, FTP1/09.
[9] K. Hashizume, M. Sugisaki, K. Htano, T. Ohmori, K. Ōgi, J. Nucl. Sci. Technol. 31 (1994) 1294.
[10] H. Saito, T. Hishi, T. Misawa, T. Ohnishi, Y. Noya, T. Matsuzaki, T. Watanabe, J. Nucl. Mater. 258–263 (1998) 1404.
[11] T. Tanabe, K. Miyasaka, T. Saze, K. Nishizawa, T. Kobayashi, T. Hayashi, M. Nishi, Fus. Sci. Technol. 41 (2002) 528.
[12] H. Saito, H. Homma, Y. Noya, T. Ohnishi, Fus. Sci. Technol. 41 (2002) 536.
[13] K. Hashizume, Y. Saruwatari, T. Hirano, T. Otsuka, T. Tanabe, in: Proceedings of the 2005 Water Reactor Fuel Performance Meeting, 2005, p. 1053.
[14] N.J. Heo, T. Nagasaka, T. Muroga, J. Nucl. Mater. 325 (2004) 53.